RAPID COMMUNICATIONS

PHYSICAL REVIEW B VOLUME 37, NUMBER 13 1 MAY 1988

Hot-electron diffusion lengths in the rare-gas solids

E. Gullikson
Center for X-Ray Optics, University of California, Lawrence Berkeley Laboratory, Berkeley, California 94720
(Received 21 December 1987)

Measurements of the secondary-electron escape probability have been used to determine the escape depth of hot electrons in thin films of Ne, Ar, and Xe. The electrons were generated with 5.9-keV x rays, and the data were analyzed using a diffusion model including absorption at the substrate. The escape depths are measured to be 0.23, 0.45, and 25 μm for Xe, Ar, and Ne, respectively, and appear to be limited by trapping at defects. It is demonstrated that the long escape depths make the rare-gas solids efficient photocathodes for x rays.

It has been shown that the escape depth of hot electrons in the rare-gas solids (RGS) is very long.[1] However, in the previous experimental measurements,[1] the hot electrons were generated at the interface of the rare-gas film and the substrate where reabsorption of the electrons at the substrate is important. Here the hot electrons are generated in the bulk of the film using 5.9-keV x rays, so the measurements are less sensitive to the substrate. Values of the hot-electron escape depth or diffusion length L for Ne, Ar, and Xe are reported here which are even longer than indicated by previous measurements. A film of Ne was grown with a diffusion length of 25 μm a value 50 times larger than in Ref. 1. It appears that at least for Ar and probably also Ne and Xe the electron diffusion length is limited by trapping at defects. Since the yield of secondary electrons produced by x rays[2] is proportional to NL/λ_x where N is the average number of secondary electrons produced per absorbed x ray, and λ_x is the x-ray attenuation length, it is demonstrated that the RGS make efficient x-ray photocathodes. Xe is over 5 times more efficient than CsI, the current photocathode of choice for applications in streak cameras[2] and position-sensitive detectors for astrophysical applications.[3]

In Fig. 1, the measurements taken from Ref. 1 are reproduced along with fits to the data made using the diffusion model with absorbing boundaries as described below. In these experiments, electrons were excited at the Au substrate by ultraviolet light with energy less than the band gap of the RGS. The electron current was measured as a function of RGS film thickness. It is evident that the decrease in the yield can be fitted with a large range of values of the electron diffusion length, the decrease in yield being mainly due to reabsorption of electrons at the Au substrate. In the limit of large L, the yield should decrease as the inverse of the film thickness. Thus, it appears that while these measurements show that L is very long they provide only a lower limit to its value.

The experimental arrangement is shown in the inset of Fig. 2. The RGS film is grown on a Be foil which is mounted on a continuous-flow liquid-He cryostat. X rays (5.9 keV) from a 100-μCi ^{55}Fe source are incident on the film through the 250-μm-thick Be substrate. Secondary electrons which leave from the opposite side of the film are guided by a magnetic field to a microchannel plate (MCP) where they are detected. The entire apparatus is enclosed in an ultrahigh vacuum chamber with a base pressure of 2×10^{-10} Torr. The films were grown by leaking the rare gas into the vacuum system until the pressure was $\approx10^{-5}$ Torr. The area of the film is defined by a 2.4-mm-diam hole in a 400-μm-thick Cu foil. The ^{55}Fe source was located 8 mm behind the Be foil, and the x-ray intensity at the RGS film was about 2×10^{4} photons/sec. The thickness of the RGS film was determined by measuring the transmitted x rays using a channel electron multiplier with a Be window which could be inserted directly in front of the cold finger. The energy spectrum of the secondary electrons was obtained using the retarding field method by biasing a set of electrodes located between the film and the MCP.

In Fig. 2, the measured detection efficiency is plotted versus thickness for an Ar film. The detection efficiency is defined here to be the fraction of x rays incident on the film which result in a count at the MCP. The data are analyzed with the following model. An x ray which is ab-

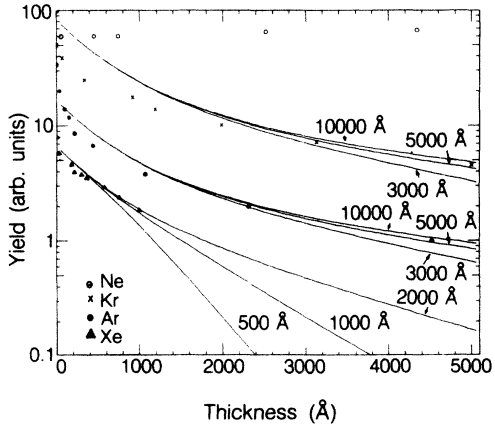

FIG. 1. Photoexcited electron yield from an Au substrate vs thickness of the RGS overlayer, from Ref. 1. The solid lines were calculated from the diffusion model discussed in the text using the values of the diffusion length shown.

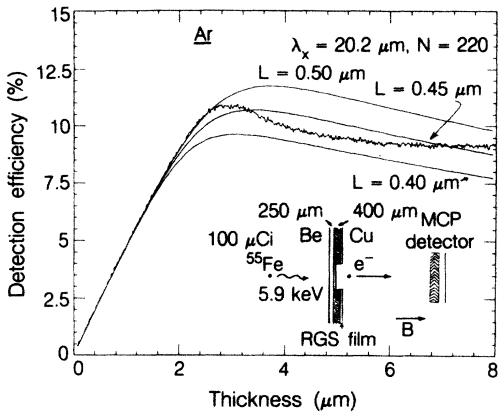

FIG. 2. X-ray detection efficiency vs film thickness for a solid Ar photocathode and 5.9-keV x rays. The solid lines were calculated using the model described in the text with the x-ray attenuation length, $\lambda_x = 20.2$ μm and the number of secondary electrons per photon, $N = 220$, and the electron diffusion length L with the values indicated. The experimental arrangement is shown in the inset.

sorbed in the film produces an energetic photoelectron. This photoelectron and the Auger electron resulting from the decay of the remaining hole both lose their energy to produce electron-hole pairs in a distance short compared with the attenuation length for the x rays, λ_x. The resulting secondaries then undergo a random walk in the film until they are trapped or escape through either surface. It is assumed that the motion of the secondary electrons can be described by the one-dimensional diffusion equation

$$\partial n/\partial t = D\partial^2 n/\partial z^2 - n/\tau \ , \tag{1}$$

where $n(z,t)$ is the electron density distribution in the film, D is the hot-electron diffusion constant, and τ is the lifetime of an electron before it is trapped. The initial electron distribution is taken to be

$$n(z,0) = Np(z) = Ne^{-z/\lambda_x}/\lambda_x \ , \tag{2}$$

where $p(z)$ is the distribution of absorbed photons and N is the average number of secondary electrons generated by each photon. Absorbing boundaries at $z = 0, x$ are assumed and the problem is solved as in Ref. 4. The number of electrons per photon which escape through the transmission side of the film is given by

$$Y_t = \int_0^x n(z,0)G_t(z)dz = \int_0^x n(z,0)\frac{\sinh(z/L)}{\sinh(x/L)}dz \ , \tag{3}$$

where $L = (D\tau)^{1/2}$ is the electron diffusion length. The Green's function, $G_t(z)$, is the probability for an electron starting at a point z to escape through the surface at $z = x$. Thus, the probability for one or more of the N secondary electrons produced by an x ray to escape is $1-[1-G_t(z)]^N$. Therefore, the detection efficiency as defined above is given by

$$\epsilon = \int_0^x p(z)\{1-[1-\epsilon_{\rm MCP}G_t(z)]^N\}dz \ , \tag{4}$$

where $\epsilon_{\rm MCP}$ is the efficiency of the MCP. This expression was used to calculate the curves in Fig. 2 with the values for the parameters listed there and $\epsilon_{\rm MCP} = 0.6$. For small film thicknesses, the efficiency is x/λ_x, since every absorbed photon results in at least one electron reaching the MCP. The initial slope was used to calibrate the rate of incident x rays and was in agreement with the rate measured directly using a NaI detector.

In Fig. 3, the detection efficiency is plotted versus film thickness for solid Xe. This film was grown at a pressure of 4×10^{-6} Torr and temperature of 35 K. Films grown at lower temperatures had lower efficiencies and corresponding shorter diffusion lengths, presumably due to a higher concentration of defects. The calculated efficiency for CsI is also shown for comparison. The highest efficiency obtained with Xe is more than 5 times that of CsI at this x-ray energy.

In Fig. 4, the secondary-electron energy distribution curves are shown versus the component of energy normal to the film. The solid line is the integral distribution $N(E)$, obtained by the retarding field method, and the dots are the differential distribution dN/dE, obtained by numerically differentiating the integral spectrum. The Ar film was 5.0μm thick and was grown at $T = 17$ K. The Xe film was 1.2μm thick and was grown at $T = 33$ K. The inelastic threshold $E_{\rm th}$ is indicated for both Ar and Xe. Above this energy, exciton production is possible.[1] Below this threshold, the only inelastic process available to an electron is the generation of phonons. It is because of the small phonon energies (< 10 meV) and the weak electron-phonon coupling in the RGS that the diffusion length is so long. The full width at half maximum (FWHM) of the energy distribution curves are remarkably narrow, the FWHM for Xe is about half that of CsI. This energy spread is important in determining the time resolution of a streak camera, for an extraction field of 5 kV/mm and an energy spread of $\Delta = 0.77$ eV the time resolution[2] would be 0.6 psec. However, the time resolution of a photocathode will also be limited by the secondary-electron lifetime τ, which can be quite long for

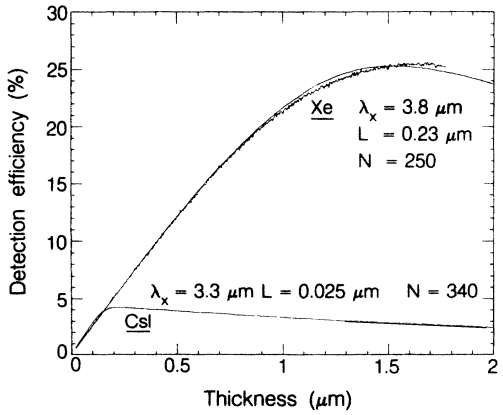

FIG. 3. The x-ray detection efficiency vs film thickness for solid Xe. The data were fitted to yield the diffusion length, $L = 0.23$ μm. The curve for CsI is shown for reference and was calculated using the electron diffusion length measured in Ref. 2.

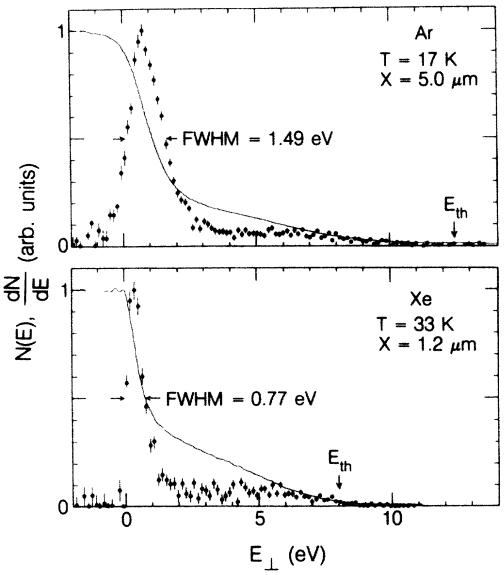

FIG. 4. Secondary-electron energy distribution curves for Xe and Ar measured at temperature T and film thickness x. The integral distribution $N(E)$ is shown as a solid line and the differential distribution dN/dE is shown as dots. The inelastic threshold E_{th} is indicated.

the RGS. For example, if we assume a mean free path of 200 Å then the diffusion constant for a 1-eV electron is 40 cm^2/sec. For Xe with a diffusion length of $L=0.2$ μm this implies an electron lifetime of $\tau=10$ psec, much longer than the time spread due to the width of the energy distribution. A diffusion length of 20 μm, observed for Ne, implies $\tau=100$ nsec.

Some relevant properties of the RGS are summarized in Table I. The average energy used to generate an electron-hole pair is E_i, and thus the average number of secondary electrons is E/E_i where E is the photon energy. All of the values of L represent lower limits since L depends on the conditions under which the film was grown. A larger diffusion length was obtained if the film was grown at higher temperature. It was also observed for Ne that the efficiency increased with time after the film was grown, this was presumably due to annealing. It is rather surprising that the diffusion length for Ar is comparable to Xe and much less than Ne. In Xe the lifetime could be

TABLE I. Properties of rare-gas solid photocathodes.

	Ne	Ar	Xe
E_a (eV)[a]	−1.3	−0.3	+0.4
λ_x (μm) at 5.9 keV[b]	118	20.2	3.8
E_i (eV)[c]		27	24
ϵ_{max} (%) at 5.9 keV	43(3)	11(1)	25.5(5)
L (μm)	25(5)	0.45(5)	0.23(5)

[a]Reference 1, Table 3.1.
[b]Reference 7.
[c]Reference 8.

the time required for a hot electron to lose enough energy so that its kinetic energy drops below the electron affinity $E_a=0.4$ eV. However, for both Ar and Ne the electron affinity is negative and some other trapping mechanism must determine τ. The observed effects of the film growth temperature on L suggests that trapping at defects limits the electron lifetime. Indeed, under similar conditions it has been shown that large vacancies exist in solid Ar.[5] Since the lifetime in Ar is much less than the thermalization time,[6] the trapping must occur for nonthermal electrons with kinetic energies ≈ 1 eV (see Fig. 4). We note that the long diffusion length in Ne could explain the observed dependence of the electron yield on film thickness in Ref. 9 without invoking exciton breakup at the surface.

In conclusion, electron diffusion lengths have been measured for Ne, Ar, and Xe. The values obtained here should be regarded as lower limits since the diffusion length is found to depend on the conditions of film growth. It is surprising that the diffusion length for Ar is so short, and it is suggested that the electrons are being trapped at defects. Solid Xe is a very efficient x-ray photocathode and should be useful in applications requiring high efficiency and good time resolution. Solid Ne was found to have the highest efficiency and longest escape depth of the rare gases studied; however, due to its long electron diffusion time it is not expected to be a suitable photocathode for applications requiring fast time response.

It is a pleasure to acknowledge discussions with B. L. Henke, A. P. Mills, Jr., and P. M. Platzman. The support of AT&T Bell Laboratories where this work was performed is gratefully acknowledged.

[1]N. Schwentner, E.-E. Koch, and J. Jortner, *Electronic Excitations in Condensed Rare Gases,* Springer Tracts in Modern Physics, Vol. 107 (Springer-Verlag, Berlin, 1985), p. 203.

[2]B. L. Henke, J. P. Knauer, and K. Premaratne, J. Appl. Phys. **52**, 1509 (1981).

[3]E. Kellogg, P. Henry, S. Murray, L. Van Speybroeck, and P. Bjorkholm, Rev. Sci. Instrum. **47**, 282 (1976).

[4]D. M. Chen, K. G. Lynn, R. Pareja, and B. Nielsen, Phys. Rev. B **31**, 4123 (1985).

[5]D. M. Schrader, A. Loewenschuss, J. Y. Jean, K. Nakamoto, and B. D. Pollard, in *Positron Annihilation,* edited by P. G. Coleman, S. C. Sharma, and L. M. Diana (North-Holland, Amsterdam, 1982), p. 657.

[6]U. Sowada, J. M. Warman, and M. P. de Haas, Phys. Rev. B **25**, 3434 (1982).

[7]B. L. Henke, P. Lee, T. J. Tanaka, R. L. Shimabukuro, and B. K. Fujikawa, At. Data Nucl. Data Tables **27**, 1 (1982).

[8]W. E. Spear and P. G. le Comber, in *Rare Gas Solids, Vol. 2,* edited by M. L. Klein and J. A. Venables (Academic, London, 1977), p. 1136.

[9]D. Pudewill, F. J. Himpsel, V. Saile, N. Schwentner, N. Skibowski, E. E. Koch, and J. Jortner, J. Chem. Phys. **65**, 5226 (1976).